

Conference materials

UDC 620.1.08, 681.786.5, 681.7.014.3

DOI: <https://doi.org/10.18721/JPM.183.143>

## **Profile construction and determination of geometric parameters of the rolling surface of a railway wheel using a laser profilometer**

K.G. Arinushkina<sup>1, 2</sup>✉, I.Yu. Savelev<sup>2</sup>, V.V. Davydov<sup>3</sup>,

A.S. Adadurov<sup>4</sup>, P.I. Tsomaev<sup>2</sup>

<sup>1</sup> Bonch-Bruevich Saint-Petersburg State University of Telecommunications,  
St. Petersburg, Russia;

<sup>2</sup> JSC "Scientific Research and Design Institute of Informatization, Automation and  
Communication in Railway Transport" (JSC "NIIAS"), Moscow, Russia;

<sup>3</sup> Peter the Great St. Petersburg Polytechnic University, St. Petersburg, Russia;

<sup>4</sup> Petersburg State Transport University, St. Petersburg, Russia

✉ [k-arinushkina@mail.ru](mailto:k-arinushkina@mail.ru)

**Abstract.** The problems arising in the processing of optical images formed from laser signals reflected from the surface of a railway wheel are considered. A design has been developed for the placement of laser emitters and photodetector devices for examining railway wheels in motion. A new algorithm has been developed aimed at improving the accuracy of constructing the profile of the rolling surface of the wheel. To process the recorded optical images in the laser radiation reflected from the surface of the wheel, a new technique based on the use of data filtering has been proposed, which uses a new algorithm that allows removing glare (a cloud of points with false data), outliers (single false points) and leaving only the necessary profile points. The new algorithm is based on the HDBSCAN (Hierarchical Density-Based Spatial Clustering of Applications with Noise) clustering algorithm. The algorithm makes it possible to exclude points forming errors during the construction of the profile of the rolling surface of the wheel. The use of a new design for the placement of optical elements and an algorithm made it possible to increase the accuracy of measurements of key wheel parameters, such as thickness, height and steepness of the ridge, and uniform rolling.

**Keywords:** laser radiation, reflected signal, optical image, matrix photodetector, wheel pair profile, surface, defects

**Citation:** Arinushkina K.G., Savelev I.Yu., Davydov V.V., Adadurov A.S., Tsomaev P.I., Profile construction and determination of geometric parameters of the rolling surface of a railway wheel using a laser profilometer, St. Petersburg State Polytechnical University Journal. Physics and Mathematics. 18 (3.1) (2025) 214–221. DOI: <https://doi.org/10.18721/JPM.183.143>

This is an open access article under the CC BY-NC 4.0 license (<https://creativecommons.org/licenses/by-nc/4.0/>)

Материалы конференции

УДК 620.1.08, 681.786.5, 681.7.014.3

DOI: <https://doi.org/10.18721/JPM.183.143>

## **Построение профиля и определение геометрических параметров поверхности катания железнодорожного колеса с помощью лазерного профилометра**

К.Г. Аринушкина<sup>1, 2</sup>✉, И.Ю. Савельев<sup>2</sup>, В.В. Давыдов<sup>3</sup>,

А.С. Агадуров<sup>4</sup>, П.И. Цомаев<sup>2</sup>

© Arinushkina K.G., Savelev I.Yu., Davydov V.V., Adadurov A.S., Tsomaev P.I., 2025. Published by Peter the Great St. Petersburg Polytechnic University.



<sup>1</sup>Санкт-Петербургский государственный университет телекоммуникаций  
им. проф. М.А. Бонч-Бруевича, Санкт-Петербург, Россия;

<sup>2</sup>АО «Научно-исследовательский и проектно-конструкторский институт информатизации,  
автоматизации и связи на железнодорожном транспорте» (АО «НИИАС»),  
Москва, Россия;

<sup>3</sup>Санкт-Петербургский политехнический университет Петра Великого,  
Санкт-Петербург, Россия;

<sup>4</sup>Петербургский государственный университет путей сообщения  
Императора Александра I, Санкт-Петербург, Россия  
✉ karinushkina@mail.ru

**Аннотация.** Рассмотрены проблемы, возникающие при обработке оптических изображений, сформированных из отраженных от поверхности колеса железнодорожного транспорта лазерных сигналов. Разработана конструкция размещения лазерных излучателей и фотоприемных устройств для обследования колес в движении. Разработан новый алгоритм, направленный на повышение точности построения профиля поверхности катания колеса. Для обработки регистрируемых оптических изображений в отраженном от поверхности колеса лазерном излучении предложена новая методика, основанная на использовании фильтрация данных, в которой применен новый алгоритм, позволяющий удалить засветку (облако точек с ложными данными), выбросы (одиночные ложные точки) и оставить только нужные точки профиля. Новый алгоритм разработан на основе плотностного алгоритма кластеризации HDBSCAN (Hierarchical Density-Based Spatial Clustering of Applications with Noise). Алгоритм позволяет исключить точки формирующие ошибки при построении профиля поверхности катания колеса. Использование новой конструкции размещения оптических элементов и алгоритма позволило повысить точность измерений ключевых параметров колеса, таких как толщина, высота и крутизна гребня, и равномерный прокат.

**Ключевые слова:** лазерное излучение, отраженный сигнал, оптическое изображение, матричный фотоприемник, профиль колесной пары, поверхность, дефекты

**Ссылка при цитировании:** Аринушкина К.Г., Савельев И.Ю., Давыдов В.В., Агадуров А.С., Цомаев П.И. Построение профиля и определение геометрических параметров поверхности катания железнодорожного колеса с помощью лазерного профилометра // Научно-технические ведомости СПбГПУ. Физико-математические науки. 2025. Т. 18. № 3.1. С. 214–221. DOI: <https://doi.org/10.18721/JPM.183.143>

Статья открытого доступа, распространяемая по лицензии CC BY-NC 4.0 (<https://creativecommons.org/licenses/by-nc/4.0/>)

## Introduction

Traditional methods of monitoring the condition of rolling stock wheels based on manual measurements during routine maintenance demonstrate significant limitations: high labor intensity, significant time costs and insufficient accuracy [1]. These disadvantages make them ineffective for modern conditions of intensive railway operation. The use of other methods for monitoring the condition of wheels, which are successfully used in the subway [2] or in trams [3] on mainline railways, is not effective.

Modern research in the field of surface control of both rail condition and wheel design focuses on the development of optoelectronic measurement methods [4]. The use of laser systems has been recognized as the most effective approach [4–7]. This technique includes capturing images of wheelsets using matrix receivers, processing the received data with special algorithms, and automatically determining geometric parameters.

Experimental data confirm that laser measuring systems, which are used in many devices, provide the necessary accuracy with minimal processing time [8–10]. The use of optical systems on railways makes it possible to effectively solve the problems of operational control of the condition of wheelsets in real-world operating conditions, meeting modern requirements for transportation safety.

In this paper, we consider a wheel parameter monitoring system that provides automated non-contact measurement of the geometric characteristics of wheelsets for a wide range of railway rolling stock. The key feature of solving the problem considered in this paper is the ability to take measurements during the movement of the train without having to stop it, which significantly increases the effectiveness of diagnostic procedures. This required the development of a new optical image processing algorithm, as well as the modernization of the design for placing optical elements below the rail level on various sections of the railway, mainly at stations and stages.

### Materials and Methods

The developed monitoring system is based on the principle of laser triangulation and includes three key components: a high-precision laser profilometer, a multi-channel photodetector and specialized software for digital signal processing [11, 12].

The measuring complex is based on a pulsed semiconductor laser source ( $\lambda = 638$  nm) with an integrated thermal stabilization system [12]. A special feature of the design is the use of Peltier elements with a digital control controller and a precision temperature sensor mounted on a common heat-dissipating substrate with an emitter. To form the measuring field, an optical scheme for converting a laser beam into a line is used, including a collimating module for forming a parallel light flux and a spherical prism that rotates the beam into a 1.0–1.3 m long line.

The formed light plane is projected onto the controlled surface of the wheel at a given angle. The reflected radiation is recorded by a highly sensitive CMOS sensor, while the spatial distribution of the light line on the matrix carries information about the geometric parameters of the profile. The distance to the object, which complements the information about the spot's coordinate, is calculated using the formula (1).

$$L = \frac{D \cdot \sin(\alpha)}{\sin(\theta + \alpha)}. \quad (1)$$

The angle  $\theta$  is determined by changing the image on the matrix for each highlighted pixel with coordinates  $(u, v)$ .  $D$  and  $\alpha$  are set during calibration.

The optical matrix receiver is made in the format of a highly sensitive CMOS matrix with a dimension of  $n \times m$  pixels, it provides the transformation of the spatial distribution of the light line into a digital profile image in the coordinate system  $(u, v)$ . The information processing device is implemented on the basis of an industrial programmable controller, it performs data processing in real time, followed by recalculation from the pixel coordinate system to the matrix  $(u, v)$ , into the real coordinate system of the measuring object.

Built-in protection and self-diagnosis mechanisms guarantee safe operation in conditions of heavy railway traffic, and special signal processing algorithms compensate for the effects of external interference, ensuring the reliability of results in real-world operating conditions.

The method of irradiating the wheel is shown in Figure 1.

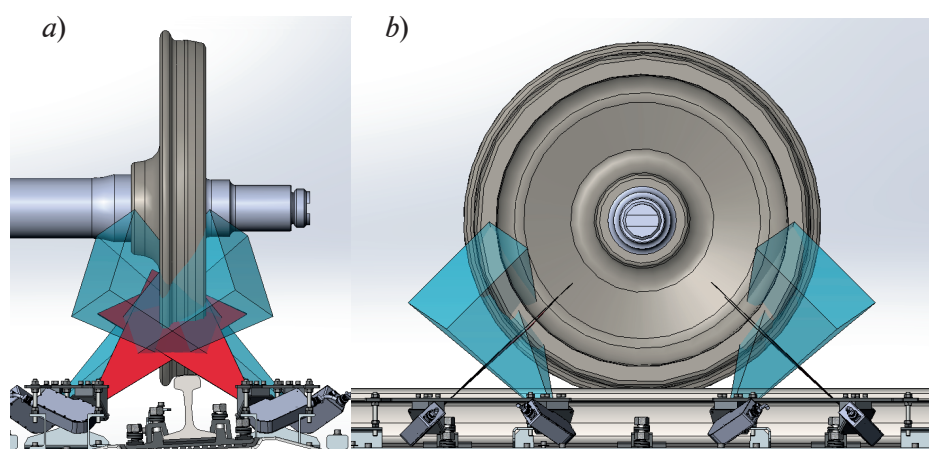


Fig. 1. The process of irradiating the wheel with profilometers side view (a), front view (b)

The outer (rolling surface) and inner sides (wheel crest) of the wheel profile are scanned separately with two profilometers pre-calibrated into one coordinate system.

The main task of the system is to measure the parameters and highlight the defects of the skating surface against the background of noise and other interference. To solve this problem, an algorithm for mathematical data processing based on the analysis of surface geometry was tested. This method analyzes the geometric parameters of the surface, such as the thickness, height and steepness of the ridge, rolling along the rolling circle and the width of the wheel rim, using laser scanning data. The known defect data is used for the analysis.

### The algorithm for filtering profile data

When processing data obtained from laser profilometers in the form of a cloud of points  $\{(x_k, y_k)\}$  (where  $k = 1 \dots N$ ), various spurious reflections can have a significant impact on the measurement accuracy, forming separate clusters of points that do not correspond to the real profile of the wheelset, and random emissions that distort the measurement results. Spurious reflections mainly occur due to the reflection of sunlight from a controlled surface, droplets of moisture or other reflective elements, creating false light signals on the receiver. Optical noise (emissions) they appear under the influence of external factors: vibration loads, electromagnetic interference, mutual influence of signals and other operational influences.

To remove outliers and spurious reflections, filtering using the density clustering algorithm HDBSCAN (Hierarchical Density-Based Spatial Clustering of Applications with Noise) is used [13, 14].

For HDBSCAN to work, two parameters need to be set: the neighborhood  $\epsilon$  is the maximum distance between data points so that they can be considered part of the same cluster, and  $m$  is the minimum number of points required to form a cluster. Two stages of clustering are performed. In the first stage, the values  $\epsilon = 5$  and  $m = 20$  are selected so as to discard outliers located at a distance greater than  $\epsilon = 5$  mm from the main point cloud. For the second stage, the values  $\epsilon = 0.5$  and  $m = 2$  are chosen so as to divide the entire point cloud into a set of clusters  $A$  and subsequently discard those clusters that do not characterize the profile. For further filtering of clusters that do not characterize the profile, the distance  $d$  between the last point of cluster  $A_i$  and the first point of cluster  $A_j$  is estimated, where  $j = i + 1$ .

$$d = \sqrt{(x_{A_{i_{end}}} - x_{A_{j_{end}}})^2 + (y_{A_{i_1}} - y_{A_{j_1}})^2}. \quad (2)$$

According to the value of the RMS error (RMSE) of the linear approximation, clusters are obtained. If  $d$  is less than 1 mm, then the points  $A_j$  of the cluster are added to  $A_i$ , the value of 1 was selected empirically. If  $d$  is greater than 1, then the standard deviation of the linear approximation of the  $N$  boundary points of the two clusters  $A_i$  and  $A_j$  is estimated. 5 points are taken from each, where the value of 5 is selected empirically. If the RMSE is less than 0.25, then the clusters are combined into one. At the end of the algorithm, there should be one, the largest cluster characterizing the profile of the railway wheel.

The values were selected based on the representation of the data and the resulting shape of the wheel profile. The threshold distance  $d = 1$  mm is close to the average Euclidean distance between neighboring points in the main cloud characterizing the rail profile. If you choose  $d \ll 1$ , the algorithm will become unnecessarily strict. Neighboring clusters that are parts of the same profile but are separated due to small noise or profilometer errors will not be combined.

If you select  $d \gg 1$  mm (for example, 3 mm), the algorithm will begin to combine the real profile and sufficiently distant parasitic reflections into one cluster, which is an error.

The value 5 is selected for the number of boundary points. If you select fewer points (1–3), the approximating line will be extremely sensitive to noise and outliers. Any “bad” point will greatly distort the tilt angle and RMSE.

If you select a large number of points (10–15), the algorithm will lose its ability to respond to local curvature. On the rounded edges of the profile (for example, the crest of the wheel), the local geometry is nonlinear.

The threshold of the deviation  $\text{RMSE} = 0.25$  was chosen based on the analysis of the approximation error of obviously continuous sections of the profile.

### The algorithm for restoring the profile and calculating its basic geometric parameters

The filtered data set is divided into  $i$  number of segments, with 10 points in each segment, and a 5-point shift between segments. A linear approximation and calculation of the average current is performed for each segment. This part of the algorithm was called piecewise linear approximation. In the end, the external and internal profiles are combined into one, taking into account the potential for rupture, that is, if necessary, a quadratic approximation of the rupture site on the wheel crest is performed.

The point cloud profile reconstruction algorithm uses a piecewise linear approximation for a set of filtered point data  $\{(x_k, y_k)\}_{k=1}^{N_f}$ , the outer and inner profiles separately, with their subsequent combination.

Each segment is approximated by a first-degree polynomial using the least squares method. The problem is reduced to solving a system of linear equations:

$$\begin{bmatrix} 1 & x_1 \\ 1 & x_2 \\ \vdots & \vdots \\ 1 & x_n \end{bmatrix} \begin{bmatrix} a_0 \\ a_1 \end{bmatrix} = \begin{bmatrix} y_1 \\ y_2 \\ \vdots \\ y_n \end{bmatrix}. \quad (3)$$

Also, the key step of the algorithm is to connect the two parts of the profile – the outside of the wheel and the inside. When data breaks in the ridge area, approximation by a second-degree polynomial is provided for a data set of the outermost 5 points from each part of the profile. If there is no gap, then the data on the ridge overlaps, since at this point the right and left halves of the profile obtained from the two profilometers are stitched.

In the end, all the coordinates are combined into the resulting matrix  $P$ :

$$P = \begin{cases} (x_i^{(outer)}, y_i^{(outer)}) \\ (x_m, \hat{y}_m), \text{ when breaking up} \\ \hat{x}_{\min}, \hat{y}_{\min}, \text{ if there is no gap} \\ (x_i^{(inner)}, y_i^{(inner)}) \end{cases}. \quad (4)$$

The basic geometric parameters shown in Table are calculated using the reconstructed profile.

### Results and Discussion

The graph of the gap approximation in the ridge area and the reconstructed wheel profile along with the dimensions are shown in Fig. 2. In this profile, there are a total of 1635 points, 359 filtered points (points from the ridge approximation are added here), 350 segments and 29 clusters.

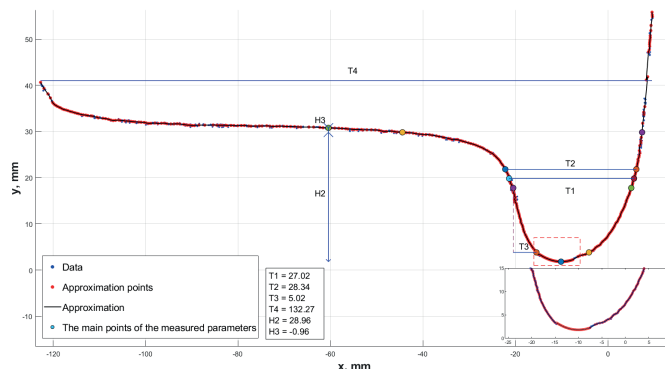


Fig. 2. Restored wheel profile: H2 – is the height of the ridge; H3 – is the rolling circle; T1 – is the thickness of the ridge at a distance of 18 mm from the top; T2 – is the thickness of the ridge at a distance of 20 mm from the top; T3 – the steepness of the ridge; T4 – the width of the rim or band.

The root-mean-square error of each segment, where  $t$  is the index of a point in the segment,  $\hat{y}_i$  is the approximated segment value, calculated using the formula:

$$\text{RMSE}_i = \sqrt{\frac{1}{n} \sum_1^n (y_t - \hat{y}_i)^2}. \quad (5)$$

In the result after averaging:  $\text{RMSE}_{\text{average}} = 0.0818 \text{ mm}$  (Fig. 3).

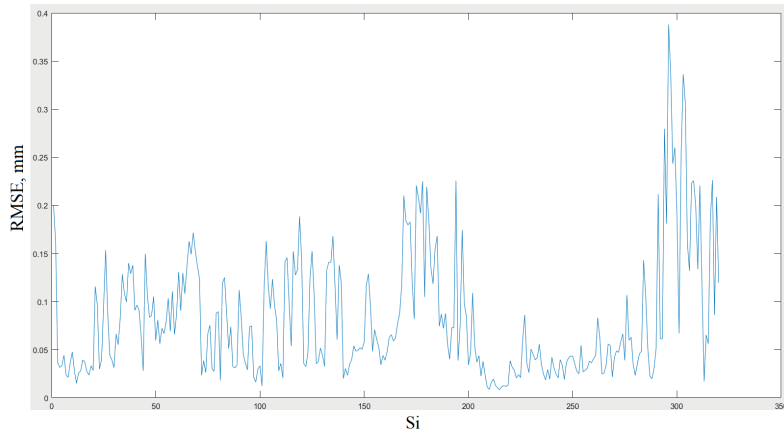


Fig. 3. Approximation error by internal profile segments

The test was carried out on a laboratory stand, the parameters were controlled using templates for monitoring and measuring the parameters of wheelsets of T-series wagons - an absolute template, universal and thickness gauge.

The laboratory wheel was measured 60 times, and based on this, the COE and confidence interval for each size were calculated using the formula:

$$\delta = \frac{t(n, p) \cdot \sigma}{\sqrt{n}}, \quad (6)$$

where, the number  $t(n, p)$  is determined by special tables of critical values of the Student's distribution points;

$\sigma$  is the mean square deviation.  $t(60, 95\%) = 2$ ;  $n = 60$ .

The results are listed in Table 1.

Table  
Geometric parameters of the wheel

| Name of the parameter                                              | The value of the parameters in mm |      |                      |                  |
|--------------------------------------------------------------------|-----------------------------------|------|----------------------|------------------|
|                                                                    | Algorithm                         | RMSE | Template measurement | Acceptable range |
| Parameter ridge thickness at a distance of 18 mm from the top - T1 | $27.02 \pm 0.07$                  | 0.23 | $27.0 \pm 0.3$       | from 24 to 33    |
| Parameter ridge thickness at a distance of 20 mm from the top - T2 | $28.34 \pm 0.06$                  | 0.19 | $28.5 \pm 0.5$       | -                |
| Parameter ridge steepness - T3                                     | $5.02 \pm 0.02$                   | 0.07 | $5 \pm 0.1$          | -                |
| The thickness of the bandage - T4                                  | $132.27 \pm 0.03$                 | 0.13 | $132 \pm 0.5$        | -                |
| Ridge height parameter - H2                                        | $28.96 \pm 0.09$                  | 0.27 | $29.0 \pm 0.1$       | -                |
| Rolling circle parameter - H3                                      | $0.96 \pm 0.01$                   | 0.03 | $1.0 \pm 0.1$        | less than 2      |

Analysis of the data obtained shows that the values of the wheel parameters do not exceed the permissible limits, therefore, this wheelset can be operated further.

The system demonstrates reliability in monitoring critical parameters of wheelsets, such as ridge height, rim thickness and rolling size, ensuring stable measurement quality at rolling stock speeds up to 120 km/h.

### Conclusion

In the course of the research, an optoelectronic monitoring system for the geometric parameters of wheelsets and track was developed and improved, adapted to work in difficult operating conditions of railway transport. Optimized operation in real conditions due to adaptability to vibrations, temperature fluctuations and precipitation. Data recovery capabilities with partial signal loss have optimized the system's performance in harsh environments.

It was possible to increase the accuracy and reliability of measurements due to the pulse mode of operation of the thermally stabilized laser, which provides resistance to external illumination, improved filtration algorithms that effectively suppress spurious reflections and noise, and an optical circuit that forms a uniform light line with high spatial resolution.

Early detection of defects (cracks, potholes, wear) with an accuracy of 0.2 mm, reduction of maintenance costs due to the transition to repairs according to the actual condition will improve the safety of rolling stock.

The prospects for further research are related to the integration of machine learning methods for automatic defect classification and prediction of the remaining life of undercarriage elements. The developed technical solutions can be scaled for use in other areas of non-destructive testing.

### REFERENCES

1. Wang N., Jia L., Zhang H., Wang Z., Zhao X., Manifold-Contrastive Broad Learning System for Wheelset Bearing Fault Diagnosis, *IEEE Transactions on Intelligent Transportation Systems*. 24 (9) (2023) 9886–9900.
2. Yan Z., Zhang H., Liu B., Zhu H., Wan H., Abnormal noise monitoring of subway vehicles based on combined acoustic features, *Applied Acoustics*. 197 (2022) 108951.
3. Jelila Y.D., Pamula W., Detection of Tram Wheel Faults Using MEMS-Based Sensors, *Sensors*. 22 (17) (2022) 6373.
4. Emoto T., Ravankar A.A., Ravankar A., Emaru T., Kobayashi Y., Wheel Surface Defect Detection Method Using Laser Sensor and Machine Vision. In proceeding 62-nd Annual Conference of the Society of Instrument and Control Engineers SICE, (2023) 1194–1199.
5. Arinushkina K.G., Overview of Fiber Optic Communications in Railway Transport: Challenges and Impact of Processing Time, In proceedings of the 2024 Conference of Young Researchers in Electrical and Electronic Engineering Elcon. (2024) 870–874.
6. Zheng F., Zhang B., Gao R., Feng Q., A high-precision method for dynamically measuring train wheel diameter using three laser displacement transducers, *Sensors*. 19 (2019) 4148.
7. Dubnischchev Y.N., Belousov P.Y., Sotnikov V.V., Belousova O.P., Optical control of the radius of a wheel rolling on a rail, *Optoelectronics, Instrumentation and Data Processing*. 48 (1) (2012) 75–80.
8. Boronenko Y., Rahimov R., Tretyakov A., Zimakova M., Petrov A., Method of Continuous Registration of Dynamic Processes of Interaction Between Rolling Stock and Railway Track, *Lecture Notes in Mechanical Engineering*. 2 (2022) 450–460.
9. Zheng Z., Song D., Xu X., Lei L., A fault diagnosis method of bogie axle box bearing based on spectrum whitening demodulation, *Sensors Switzerland*. 20 (24) (2020) 1–19.
10. Davydov V.V., Smirnov K.J., An Optical Method of Monitoring the State of Flowing Media with Low Transparency That Contain Large Inclusions, *Measurement Techniques*. 62 (6) (2019) 519–526.
11. Wang X., Lu Z., Wen J., Wei J., Wang Z., Kinematics modelling and numerical investigation on the hunting oscillation of wheel–rail nonlinear geometric contact system, *Nonlinear Dynamics*. 107 (3) (2022) 2075–2097.
12. Arinushkina K.G., Adadurov A.S., Davydov V.V., Features of the operation of a laser profilometer in an automated rolling stock control system, *St Petersburg State Polytechnical University Journal Physics and Mathematics*. 16 (3.2) (2023) 56–62.



13. **Stewart G., Al-khassaweneh M.**, An Implementation of the HDBSCAN\* Clustering Algorithm. *Applied Sciences*. 12 (2022) 2405.

14. **Bhandary P., Joyce R.J., Nicholas C.** Ransomware Evolution: Unveiling Patterns Using HDBSCAN, *Ceur Workshop Proceedings*. 3920 (2024) 174–189.

## THE AUTHORS

**ARINUSHKINA Kseniya G.**  
k-arinushkina@mail.ru  
ORCID: 0000-0002-1156-2071

**SAVELEV Igor Yu.**  
savelev.igor@mail.ru  
ORCID: 0009-0002-7511-7740

**DAVYDOV Vadim V.**  
davydov\_vadim66@mail.ru  
ORCID: 0000-0001-9530-4805

**ADADUROV Aleksandr S.**  
vorudada@mail.ru  
ORCID: 0000-0002-9520-4596

**TSOMAEV Pavel I.**  
pav.tsomaev@mail.ru  
ORCID: 0009-0002-4609-1692

*Received 15.08.2025. Approved after reviewing 11.09.2025. Accepted 24.09.2025.*